

**UNIVERSIDAD SAN FRANCISCO DE QUITO USFQ**

**Colegio de Ciencias e Ingenierías**

**Analysis of the Influence of Steel Fibers on the Shear Capacity of  
Reinforced Concrete Beams  
through Critical Shear Displacement Theory**

**David Mateo Ramírez Quincha**

**Moisés Aquiles Aray Ratti**

**Ingeniería Civil**

Trabajo de fin de carrera presentado como requisito  
para la obtención del título de  
Ingeniero Civil

Quito, 18 de diciembre de 2020

**UNIVERSIDAD SAN FRANCISCO DE QUITO USFQ**

**Colegio de Ciencias e Ingenierías**

**HOJA DE CALIFICACIÓN DE TRABAJO DE FIN DE  
CARRERA**

**Analysis of the Influence of Steel Fibers on the Shear Capacity of  
Reinforced Concrete Beams  
through Critical Shear Displacement Theory**

**David Mateo Ramírez Quincha Ramírez**

**Moisés Aquiles Aray Ratti**

**Nombre del profesor, Título académico**

**Eva Lantsoght, Dr.ir.**

Quito, 18 de diciembre de 2020

## DERECHOS DE AUTOR

Por medio del presente documento certifico que he leído todas las Políticas y Manuales de la Universidad San Francisco de Quito USFQ, incluyendo la Política de Propiedad Intelectual USFQ, y estoy de acuerdo con su contenido, por lo que los derechos de propiedad intelectual del presente trabajo quedan sujetos a lo dispuesto en esas Políticas.

Asimismo, autorizo a la USFQ para que realice la digitalización y publicación de este trabajo en el repositorio virtual, de conformidad a lo dispuesto en el Art. 144 de la Ley Orgánica de Educación Superior.

Nombres y apellidos: David Mateo Ramírez Quincha

Código: 00130809

Cédula de identidad: 1722732995

Lugar y fecha: Quito, 18 de diciembre de 2020

Nombres y apellidos: Moisés Aquiles Aray Ratti

Código: 00134657

Cédula de identidad: 1310070055

Lugar y fecha: Quito, 18 de diciembre de 2020

## **ACLARACIÓN PARA PUBLICACIÓN**

**Nota:** El presente trabajo, en su totalidad o cualquiera de sus partes, no debe ser considerado como una publicación, incluso a pesar de estar disponible sin restricciones a través de un repositorio institucional. Esta declaración se alinea con las prácticas y recomendaciones presentadas por el Committee on Publication Ethics COPE descritas por Barbour et al. (2017) Discussion document on best practice for issues around theses publishing, disponible en <http://bit.ly/COPETHeses>.

## **UNPUBLISHED DOCUMENT**

**Note:** The following capstone project is available through Universidad San Francisco de Quito USFQ institutional repository. Nonetheless, this project – in whole or in part – should not be considered a publication. This statement follows the recommendations presented by the Committee on Publication Ethics COPE described by Barbour et al. (2017) Discussion document on best practice for issues around theses publishing available on <http://bit.ly/COPETHeses>.

## RESUMEN

El concreto reforzado con fibras de acero (SFRC) representa un gran avance en tecnologías del hormigón, pero su uso ha quedado relegado a elementos no estructurales debido a la falta de estudios y métodos de cálculo de sus propiedades mecánicas.

Nuestro trabajo busca analizar la efectividad del método de cálculo de la capacidad a corte en vigas a través de los mecanismos portadores de cortante del SFRC usando la teoría de desplazamiento crítico (CSDT) propuesta por Yang y su capacidad a flexión.

Definir otro método de cálculo que incluya las propiedades y respuestas mecánicas del SFRC mejorará el desempeño de los mecanismos y límites de falla de los elementos estructurales, permitiendo su diseño y mayor adopción. Esto ayudaría a reemplazar o mejorar los métodos empíricos utilizados en los estándares actuales.

Para obtener resultados comparamos la experimentación con elementos que cumplen con:  $a/d \geq 2.5$  y  $\rho = 1 \mp 0.5\%$ . Obteniendo resultados con errores significativos, pero que mostraran resultados consistentes con los valores de la experimentación.

El resultado de desarrollar esta teoría nos permitió determinar que este enfoque de cálculo esté cerca de la realidad, pero necesitará ajustes futuros con nuevos datos de experimentación para proporcionar resultados que excedan la precisión de los métodos empíricos comunes.

Palabras clave: fibras de acero, desplazamiento crítico, cortante, mecanismos de corte, límites de falla, ancho de agrietamiento.

## ABSTRACT

Steel fiber reinforced concrete (SFRC) represents a great advancement of concrete technology, but its use has been relegated to non-structural elements due to the lack of studies and calculation methods of its mechanical properties.

Our work seeks to analyze the effectiveness of the calculation method of shear capacity in beams through the analysis of the shear carrying mechanisms using critical shear displacement theory (CSDT) proposed by Yang (2016) and their flexural capacity.

Defining another calculation method that includes the properties and mechanical responses of SFRC will improve the performance of the mechanisms and failure limits of structural elements, allowing its design and greater adoption. This could help to replace or improve the empirical methods used in current standards.

To obtain results we compare the experimentation with elements that comply with:  $a / d \geq 2.5$  and  $\rho = 1 \mp 0.5\%$ . Obtaining results with significant errors, but consistent with experimental values.

The result of developing this theory allowed us to determine that this calculation approach is close to reality but will need future adjustments with new experimentation data to provide results that exceed the precision of common empirical methods.

Key words: Steel fibers, critical shear displacement, shear, shear carrying mechanisms, failure limits, crack width.

## TABLE OF CONTENT

<b>HOJA DE CALIFICACIÓN DE TRABAJO DE FIN DE CARRERA .....</b>	<b>1</b>
<b>DERECHOS DE AUTOR .....</b>	<b>2</b>
<b>ACLARACIÓN PARA PUBLICACIÓN .....</b>	<b>3</b>
<b>UNPUBLISHED DOCUMENT .....</b>	<b>3</b>
<b>RESUMEN .....</b>	<b>4</b>
<b>ABSTRACT .....</b>	<b>5</b>
<b>TABLE OF CONTENT .....</b>	<b>6</b>
<b>TABLE INDEX .....</b>	<b>7</b>
<b>FIGURES INDEX .....</b>	<b>8</b>
<b>INTRODUCTION .....</b>	<b>9</b>
<b>LITERATURE REVIEW .....</b>	<b>11</b>
<i>Critical shear displacement theory .....</i>	<i>11</i>
<i>Shear carrying mechanisms of reinforced concrete without shear reinforcement .....</i>	<i>12</i>
<b>METHODS .....</b>	<b>14</b>
<i>Image Correction for DIC .....</i>	<i>14</i>
<i>Critical Shear Displacement Theory extended for Steel Fiber Reinforced Concrete .....</i>	<i>15</i>
<i>Flexural Equilibrium .....</i>	<i>15</i>
<i>Tension Across Crack .....</i>	<i>20</i>
<i>Aggregate Interlock .....</i>	<i>21</i>
<i>Dowel Action .....</i>	<i>22</i>
<i>Shear Capacity .....</i>	<i>26</i>
<b>RESULTS .....</b>	<b>28</b>
<b>DISCUSSION .....</b>	<b>29</b>
<b>SUMMARY AND CONCLUSIONS .....</b>	<b>31</b>
<b>NOTATION LIST .....</b>	<b>33</b>
<b>BIBLIOGRAPHIC REFERENCES .....</b>	<b>36</b>
<b>APENDIX A .....</b>	<b>38</b>
<b>APENDIX B .....</b>	<b>39</b>
<b>APENDIX C .....</b>	<b>40</b>
<i>MathCAD Code .....</i>	<i>40</i>

**TABLE INDEX**

Table 1 Equations for CSDT .....	13
Table 2 Equations for cracking moment .....	17
Table 3 Equations for flexural equilibrium .....	17
Table 4 Equations for tension across crack .....	21
Table 5 Equations for aggregate interlock .....	22
Table 6 Equations for dowel action.....	24
Table 7 Equations for shear capacity CSDT .....	26
Table 8 Statistical properties of <b>tested capacity/predicted capacity</b> for considered experiments according to different authors, with <b>AVG = average</b> , .....	28
Table 9 Results for SFRC using CSDT .....	38
Table 10 Statistical properties of <b>tested capacity/predicted capacity</b> for considered experiments according to different authors, with <b>AVG = average</b> , .....	39



## FIGURES INDEX

Figure 1 Basic imaging model .....	14
Figure 2 Simulink Arrangement MATLAB .....	15
Figure 3 Thorenfeldt Stress-Strain Diagram .....	16
Figure 4 Element, Stress and Strain Diagrams .....	16
Figure 5 Flow chart for finding the neutral axis.....	20
Figure 6 Stress model for tension across crack .....	21
Figure 7 Dowel action effect (Lima de Resende, Cardoso, & Shehata, 2020) .....	23
Figure 8 Actual behavior of fibers (Lima de Resende, Cardoso, & Shehata, 2020).....	23
Figure 9 Proposed model (Lima de Resende, Cardoso, & Shehata, 2020) .....	23
Figure 10 Direct Shear transfer in the concrete compressive zone .....	26
Figure 11 Shear capacity for SFRC using CSdT.....	27

## INTRODUCTION

Concrete and reinforced concrete are widely used as building construction materials on most countries due to its ease of use and properties. Mechanically, concrete is strong in compression and weak in tension (Wight & MacGregor, 2012) That is why reinforcement is crucial on concrete elements subjected to flexure and shear to carry most of the tension and avoid collapse. A great option to improve the mechanical properties of concrete is to use dispersed steel fibers as part of the mixture. Although there are a lot of mechanical advantages of steel fiber reinforced concrete (SFRC), it is not well adopted by construction codes.

One of the most important effects that reinforced concrete must fight is the shear failure due to the size of shear loads transferred to elements like beams. Traditionally, shear loads are carried mostly by shear reinforcement such as stirrups, but they require a great amount of steel and increase the overall weight of elements. Since shear capacity has been evaluated with empirical approaches on codes as ACI's, determining the shear capacity of members without shear reinforcement would be considered as an important topic in structural design (Yang, Uijl, & Walraven, 2016). A great way for determining the shear capacity of a beam is by analyzing the shear carrying contributions of different mechanisms like the concrete in the compression zone  $V_c$ , the dowel action of the flexural reinforcement  $V_d$  and the friction between aggregates inside a shear crack  $V_{ai}$ . Another mechanism that is important to consider in the case of SFRC is the tension across the crack  $V_f$  due to the fibers bridging the crack and transferring tension (Lantsoght E. O., 2019). For SFRC, there are not well established theoretical models that calculate the shear capacity but is possible to tweak the already developed expressions of shear carrying mechanisms to include this effect.

The aim of this research is to develop expressions that calculate the shear capacity for each mechanism of SFRC to facilitate design of members using this material and to know exactly how each mechanism benefits by the properties and distribution of steel fibers. These

expressions could also be used on digital image correlation (DIC) software to predict the capacity of a SFRC member just by analyzing the crack displacement on a series of pictures of a tensile strength test (four-point bending test).

## LITERATURE REVIEW

### *Critical shear displacement theory*

The scope of this theory is to create an alternative to the empirical methods for the analysis and design of concrete structures given in commonly used codes and based on relatively common concrete elements. As an option for the analysis of structures composed of materials of greater resistance and structural elements with specific and unusual dimensions, a model was idealized to analyze the physical and mechanical mechanisms of concrete elements.

As the main point of this analysis, the crack width is defined as the main lower bound of this model, relating it to the different mechanisms that act during the loading of a concrete element. This analysis will focus on the behavior of concrete elements, mainly their shear forces, without the presence of transverse reinforcements. The CSdT considers a concrete state in which a main flexural crack reaches a critical point of stress that leads to the formation of a shear failure Crack, and therefore 2 common failure mechanisms: flexural shear failure (opening of the critical inclined crack) and shear compression failure (beam does not fail immediately but by the crushing of concrete on the compression zone. For the flexural shear failure state, 3 main mechanisms of shear resistance can be observed: the direct shear transfer in the concrete compressive zone  $V_c$ , the aggregate interlock  $V_{ai}$ , and the dowel action  $V_d$  (Yang, Uijl, & Walraven, 2016).

Furthermore, a simplified model was developed that would describe in a quantifiable and measurable way the behavior of shear-generated cracking. There are two defined stages in the formation of the failure system, the main critical shear crack, and the secondary cracking in the steel reinforcement, progressively increasing the width of both cracks. The shear displacement of a flexural crack is influenced by the Shear force, the bending moment, and the

profile of the crack at the cracked cross-section. The profile of a flexural crack is determined by the ratio between the moment and the shear force  $M/Vd$ . This parameter will define the behavior of the faults and the shear resistance offered by the analyzed element.

For common elements of concrete and corrugated reinforcement, the second failure mechanism is the most common, thus defining the crack spacing as the space between a fully developed crack and the next possible cracked section  $l_{cr,m}$  Eq. (1). The main shear crack width at the longitudinal reinforcement level is obtained by multiplying the crack spacing with the strain in the steel Eq. (2). Finally, the critical shear displacement between the crack faces is obtained with Eq. (3). Eq. (1), (2) and (3) define the simplified crack profile proposed by (Yang, Uijl, & Walraven, 2016).

### ***Shear carrying mechanisms of reinforced concrete without shear reinforcement***

In a cracked reinforced concrete element without stirrups, the shear force is transferred through the cross section by the three already mentioned mechanisms and the total shear capacity  $V$  is determined by the sum of the effects Eq. (4). To simplify design, a simplified crack profile was defined taking the main crack as a vertical line which height is defined as  $s_{cr}$  Eq. (5) and the crack spacing as  $w_b$  Eq. (2). Finally, an experimental expression for the crack width was developed by Yang that depends on the effective depth and the longitudinal bar diameter Eq. (3) (2016). To calculate the capacity an iterative process is required by varying the value for the ultimate shear capacity until is equal to the value obtained in Eq. (4).

Table 1 Equations for CSDT

Title	Equation	#
	$l_{cr,m} = \frac{S_{cr}}{k_c}$	(1)
	$w_b = l_{cr,m} \varepsilon_s$	(2)
	$\Delta_{cr} = \frac{25d}{29800\phi} \text{mm} + 0.005\text{mm} \leq 0.025\text{mm}$	(3)
	$V = V_c + V_{ai} + V_d$	(4)
<b>Critical Shear Displacement Theory</b>	$s_{cr} = \left[ 1 + \rho_s * n_e - \sqrt{2\rho_s * n_e + (\rho_s * n_e)^2} \right] * d$	(5)
	$V_{ai} = f'_c{}^{0.56} * b * s_{cr} \frac{0.03}{w_b[\text{mm}] - 0.01} (-978\Delta_{cr}^2 + 85\Delta_{cr} - 0.27) \text{ [kN]}$	(6)
	$V_c = \frac{2}{3} * \frac{z_c}{z} * V = \frac{d - s_{cr}}{d + 0.5s_{cr}} * V \text{ [kN]}$	(7)
	$V_d = 1.64 * b_n * \phi * \sqrt[3]{f_c} \text{ [kN]}$	(8)

## METHODS

### *Image Correction for DIC*

The first approached assignment was the correction of sets of images taken during a four-point bending test of a SFRC that could be used on a DIC software. Many of these images were taken in an angle that most known DIC software could not recognize. To correct these images, it was required a projective transformation that uses a transformation matrix to displace a set of pixels from a plane to another. The issue lies when correcting the whole set of images, since the member is deformed until failure, bringing a changing set of pixels from one plane to another required the generation of multiple transformation matrices, because applying the same initial matrix would have taken only into consideration the image space of the undeformed member.

$$\begin{bmatrix} x' \\ y' \\ 1 \end{bmatrix} \cong \begin{bmatrix} wx' \\ wy' \\ w \end{bmatrix} = \begin{bmatrix} a & b & c \\ d & e & f \\ g & h & i \end{bmatrix} \begin{bmatrix} x \\ y \\ 1 \end{bmatrix}$$

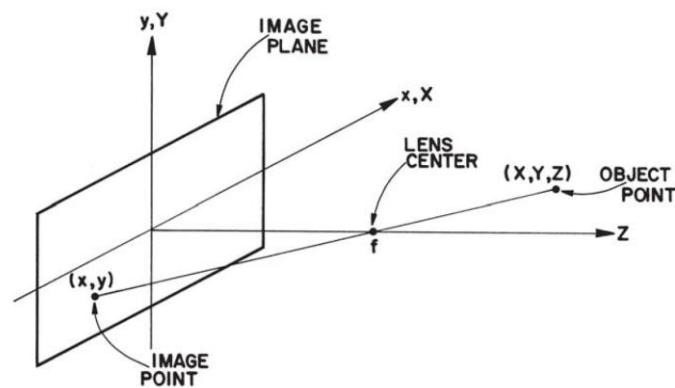


*Figure 1 Basic imaging model*

We decided to use the Simulink software, part of MATLAB, specifically the Computer Vision System Toolbox to design an arrangement that allowed us to correct the images in an individual manner. As inputs we had the original image, and two matrix that show us points of

reference to generate a Geometric transformation matrix. The output was an image corrected in base of the desired point adjustments.

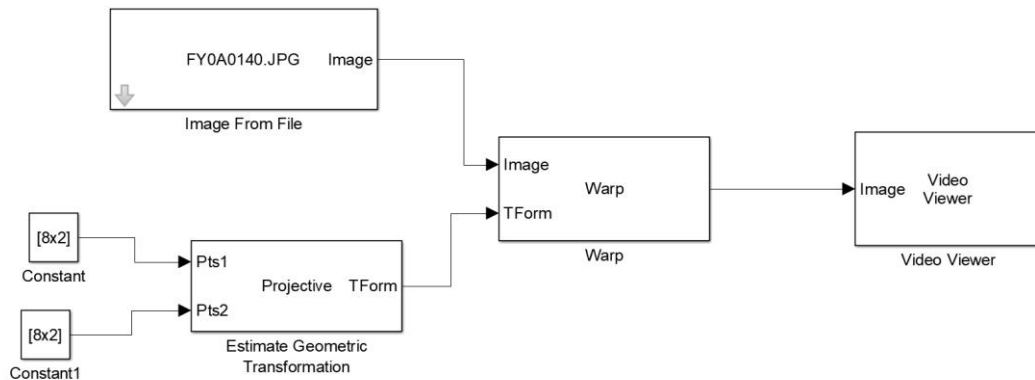


*Figure 2 Simulink Arrangement MATLAB*

As a result of the application of this method of correction, we obtained a transformed image, but this modification was not significant enough to completely correct the projection effect. It would be advisable to apply the same approach, deepening in the development of a geometric transformation matrix that could achieve something closer to the expected results. It will be necessary a more in-depth research and development in the subject of Digital Image Processing.

### ***Critical Shear Displacement Theory extended for Steel Fiber Reinforced Concrete***

#### ***Flexural Equilibrium***

To calculate the shear capacity in SFRC through CSDT, finding the strain in the longitudinal reinforcement and the distance to the neutral axis is required. Through equilibrium these two values can be calculated. Since the only input given is the external moment, an iterative process is done as seen in figure 5. A big assumption considered for the calculations was that there is a linear relation of the moment curvature diagram between cracking and yielding and between yielding and the ultimate state. Thorenfeldt's model was used for the equilibrium for the cracked and yield states (model in figures 3 and 4) (1987). On the other



hand, Whitney's model was used for the equilibrium for the ultimate state (Wight & MacGregor, 2012) by using the expressions from ACI Committee 544 to calculate the effects of the fibers as a tension block as shown in figure 4 (1999). A detailed process for the calculations is shown in figure 5.

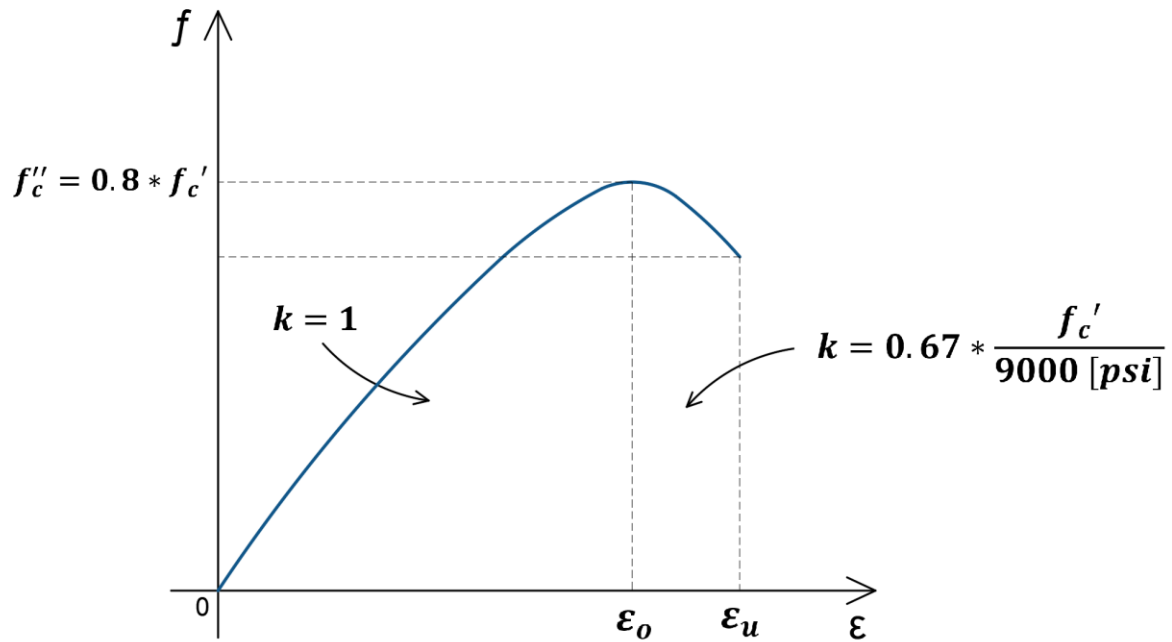


Figure 3 Thorenfeldt Stress-Strain Diagram

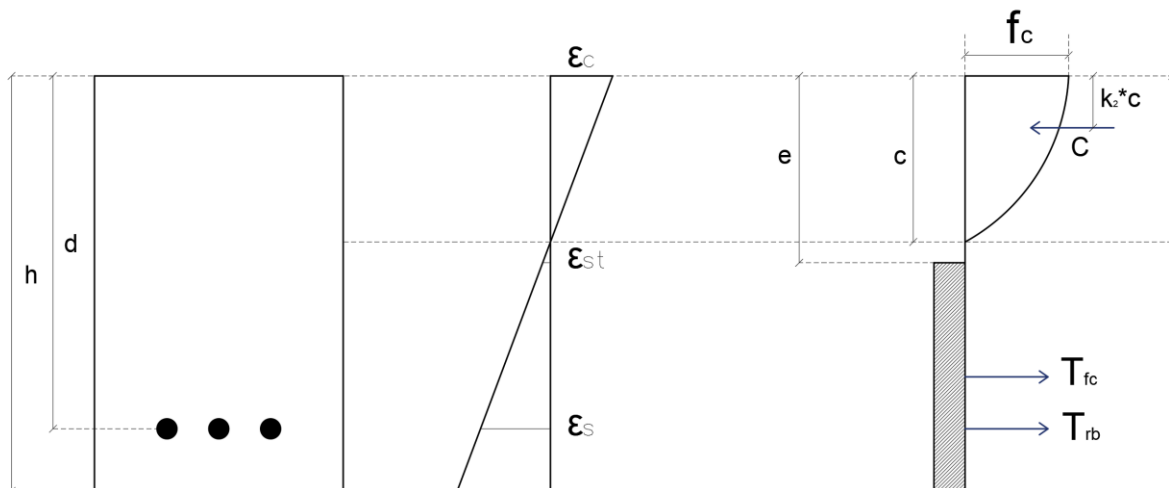


Figure 4 Element, Stress and Strain Diagrams.

Table 2 Equations for cracking moment

Title	Equation	#
<b>Cracking Moment and Curvature</b>	$RI = \frac{V_f * l_f}{d_f}$	(9)
	$f_{rf} = 0.97 * f_{cu}[MPa]^{0.5} + 0.295 * f_{cu}[MPa]^{0.5} * RI + 1.117 * RI$	(10)
	$\varepsilon_{cr} = \frac{f_{fr}}{E_c}$	(11)
	$\varepsilon_{s.cr} = \frac{\left(d - \frac{h}{2}\right)}{\frac{h}{2}} * \varepsilon_{cr}$	(12)
	$M_{cr} = \frac{f_{fr} * I_g}{\frac{h}{2}}$	(13)
	$\phi_{cr} = \frac{\varepsilon_{s.cr}}{\frac{h}{2}}$	(14)

Table 3 Equations for flexural equilibrium

Title	Equation	#
<b>Finding Yield Moment with Thorenfeldt approach</b>	$n = 0.8 + \left(\frac{f'_c}{2500[psi]}\right)$	(15)
	$\varepsilon_o = \frac{f'_c}{E_c} * \left(\frac{n}{n-1}\right)$	(16)
	$\varepsilon_y = \frac{f_y}{E_s}$	(17)
	$\varepsilon_{c.y} = \frac{\varepsilon_y}{d - c_y} * c_y$	(18)
	$\beta_{1.y} = \frac{\ln\left(1 + \left(\frac{\varepsilon_{c.y}}{\varepsilon_o}\right)^2\right)}{\frac{\varepsilon_{c.y}}{\varepsilon_o}}$	(19)

$$k_{2,y} = 1 - \frac{2 * \left( \left( \frac{\varepsilon_{c,y}}{\varepsilon_o} \right) - \text{atan} \left( \frac{\varepsilon_{c,y}}{\varepsilon_o} \right) \right)}{\left( \frac{\varepsilon_{c,y}}{\varepsilon_o} \right)^2 * \beta_{1,y}} \quad (20)$$

$$F = \frac{\left( \frac{l_f}{d_f} \right) * V_f * \rho_f}{100} \quad (21)$$

$$\sigma_t = 0.772 \text{ [MPa]} * F \quad (22)$$

$$\varepsilon_{sf} = \frac{\sigma_t}{E_c} \quad (23)$$

$$e_y = (e_{sf} + e_{cy}) * \left( \frac{c_y}{\varepsilon_{c,y}} \right) \quad (24)$$

$$\text{for } \frac{\varepsilon_{c,y}}{\varepsilon_o} \leq 1 \quad k_1 = 1 \quad (25)$$

$$\text{for } \frac{\varepsilon_{c,y}}{\varepsilon_o} > 1 \quad k_1 = 0.67 + \frac{f'_c}{9000 \text{ [psi]}} \quad (26)$$

$$C_y = \beta_{1,y} * f_c * b * c_y \quad (27)$$

$$T_y = A_s * f_y + \sigma_t * b * (h - e_y) \quad (28)$$

$$M_y = (A_s * f_y * (d - k_{2,y} * c_y)) + \sigma_t * b * (h - e_y) * \left( \frac{h}{2} + \frac{e_y}{2} - k_{2,y} * c_y \right) \quad (29)$$

$$\phi_y = \frac{\varepsilon_y}{d - c_y} \quad (30)$$

$$\beta_{1w} = 0.85 \quad \text{for } 17 \text{ [MPa]} \leq f'_c \leq 28 \text{ [MPa]}$$

$$\beta_{1w} = 0.85 - 0.05 * \left( \frac{f'_c - 28 \text{ [MPa]}}{7 \text{ [MPa]}} \right) \quad \text{for } 28 \text{ [MPa]} < f'_c < 55 \text{ [MPa]} \quad (31)$$

$$\beta_{1w} = 0.65 \quad \text{for } f'_c \geq 55 \text{ [MPa]}$$

$$\begin{aligned} & c_u * \beta_{1w} * b * f'_c * 0.85 \\ & = A_s * \left( E_s * \frac{0.003 * (d - c_u)}{c_u} \right) + \sigma_t * b \\ & * \left( h - (\varepsilon_{sf} + 0.003) * \left( \frac{c_u}{0.003} \right) \right) \end{aligned} \quad (32)$$

**Ultimate  
Moment  $M_u$**

$$a_u = \frac{A_s * f_y + \sigma_t * b * (h - e_y)}{0.85 * f'_c * b} \quad (33)$$

$$e_u = (e_{sf} + 0.003) * \left( \frac{c_u}{0.0033} \right) \quad (34)$$

$$M_u = \left( A_s * f_y * \left( d - \frac{a_u}{2} \right) \right) + \sigma_t * b * (h - e_u) * \left( \frac{h}{2} + \frac{e_u}{2} - \frac{a_u}{2} \right) \quad (35)$$

$$\varepsilon_{su} = \frac{0.003 * (d - c_{u0})}{c_{u0}} \quad (36)$$

$$\phi_u = \frac{\varepsilon_{su}}{d - c_{u0}} \quad (37)$$

*Finding steel  
strain  
corresponding to  
M<sub>ext</sub> (using M-φ  
linear  
interpolation):*

$$\varepsilon_s = \phi_{M_{ext}} * (d - c) \quad (38)$$

$$M_{T\_fiber} = \sigma_t * b * (h - e) * \left( \frac{h}{2} + \frac{e}{2} - k_2 * c \right) \quad (39)$$

$$M_{int} = M_{T\_steel} + M_{T\_fiber} \quad (40)$$

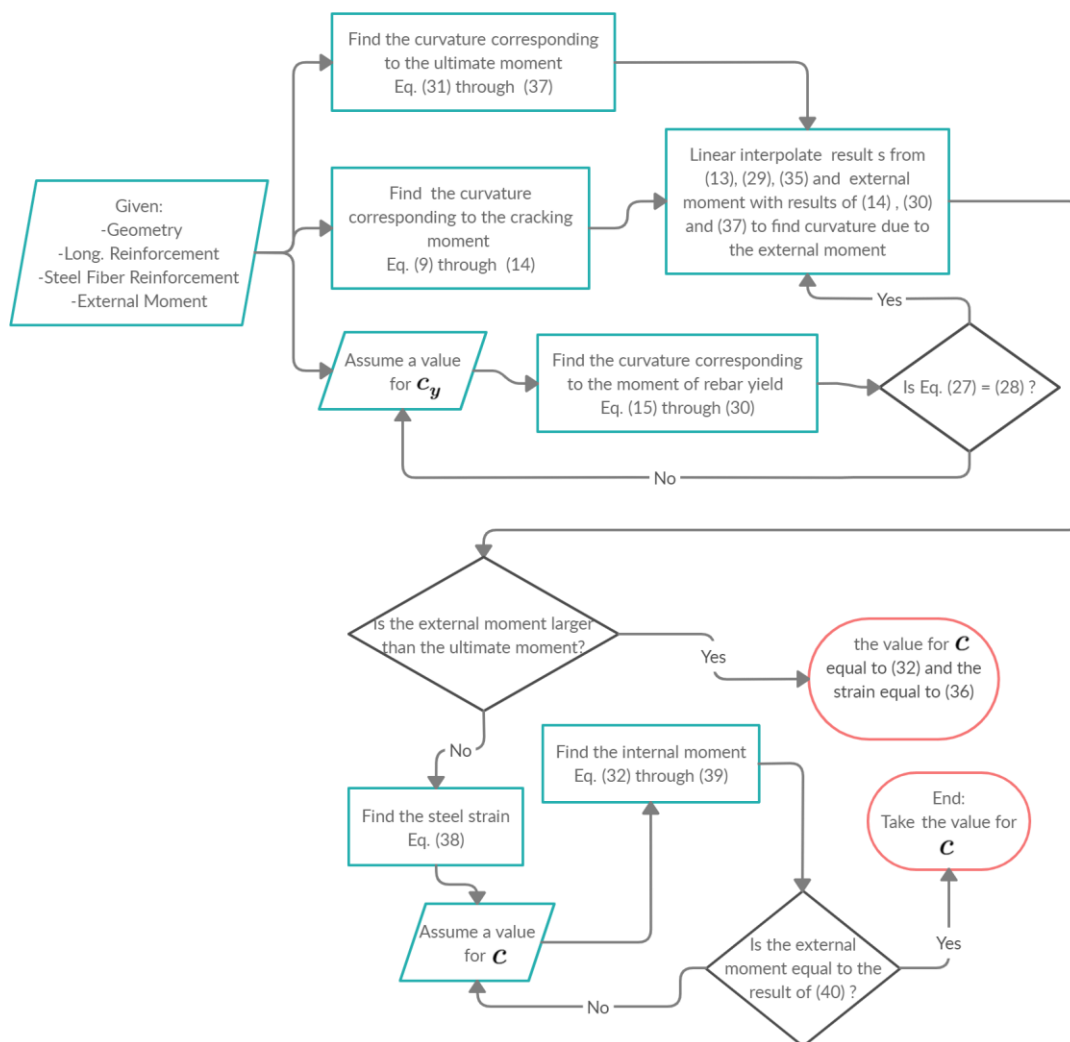


Figure 5 Flow chart for finding the neutral axis

### Tension Across Crack

This mechanism is important for SFRC because when the inclined shear crack is created, fibers bridging the crack will be able to impose resistance. The shear carried by this mechanism can be modeled as a distributed load perpendicular to the crack which vertical component corresponds to the shear stress carried by the fibers. To calculate the tension across the crack a model from (Dinh, Parra-Montesinos, & Wight, 2011) modified by (Singh & Jain, 2014) was considered (model in figure 6). The number of fibers crossing a unit area  $N$  (44) and the average pullout force per fiber  $f$  (42) are used to calculate the tensile stress resisted by the fibers

bridging a unit area of the inclined crack (45). Using these values, the shear resisted by fiber tension is obtained (46).

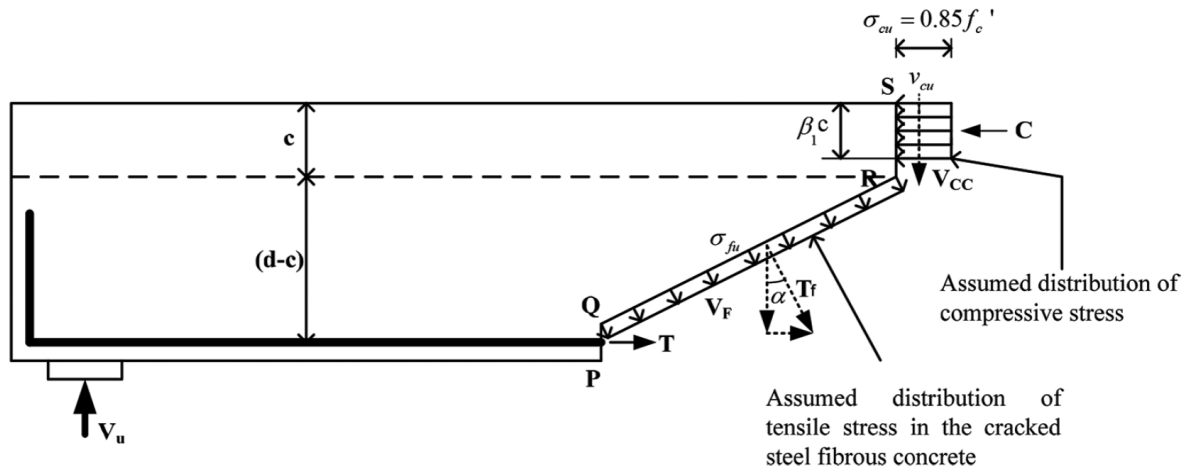


Figure 6 Stress model for tension across crack

(Singh & Jain, 2014)

Table 4 Equations for tension across crack

Title	Equation	#
<b>Tension Across Crack</b>	$\tau = 0.85 * \sqrt{f'_c} [MPa]$	(41)
	$f = \tau * \pi * D_f * d_f * \frac{l_f}{4}$	(42)
	$r_f = \frac{d_f}{2}$	(43)
	$N = 0.5 * \frac{V_f}{\pi * r_f^2}$	(44)
	$\sigma_{fu} = N * f$	(45)
	$V_F = \sigma_{fu} * b * (d - c) * \cot(\alpha)$	(46)

### Aggregate Interlock

The aggregate interlock mechanism considers the friction between aggregates in the concrete mix to provide resistance to shear. For SFRC, it is safe to say that there will be an

increased aggregate interlock capacity because the fibers reduce the size of crack width (Lantsoght E. O., 2019). On the other hand, there are not many studies regarding this mechanism for SFRC, so it will be a conservative approach to consider the same equation (6) developed by Walraven to calculate its capacity (1981). This equation depends on the steel strain and crack spacing which will have different values because of the fibers as mentioned before. Another big assumption made is that for the critical shear displacement the same expression developed by Yang was used and should not necessarily apply in the case of SFRC because it is an empirical expression based on experimental results (53).

*Table 5 Equations for aggregate interlock*

<b>Title</b>	<b>Equation</b>	<b>#</b>
<b>Aggregate Interlock</b>	$\rho_r = \frac{A_s}{2.5 * (h - d) * b}$	(47)
<b>Simplified Crack Properties</b>	$k_{1f} = 1 + \sqrt{\frac{200 [mm]}{d}}$	(48)
	$k_{2f} = 0.5 \quad (bending)$	(49)
	$l_{crm} = \left( 50 [mm] + 0.25 * k_{f1} * k_{f2} * \frac{\phi}{\rho_r} \right) * \left( \frac{50}{\frac{l_f}{d_f}} \right)$	(50)
	$s_{cr} = \left[ 1 + \rho_s n_e - \sqrt{2\rho_s n_e + (\rho_s n_e)^2} \right] d$	(51)
<b>Crack width at the level of longitudinal reinforcement</b>	$w_b = l_{crm} * \varepsilon_s$	(52)
<b>Critical Shear Displacement</b>	$\Delta_{cr} = \frac{25d}{29800\phi} + 0.005 \leq 0.025$	(53)

### Dowel Action

In SFRC, there is a noticeable improvement in dowel resistance because the fibers will reduce the width of dowel cracks (splitting cracks) by bridging in-between. To calculate the

capacity due to dowel action a beam on elastic foundation mechanism was adopted (BEF) (Lima de Resende, Cardoso, & Shehata, 2020). This will help us calculate  $V_d$  using moment equilibrium. The mechanical proposed model is presented in figures 7, 8 and 9.

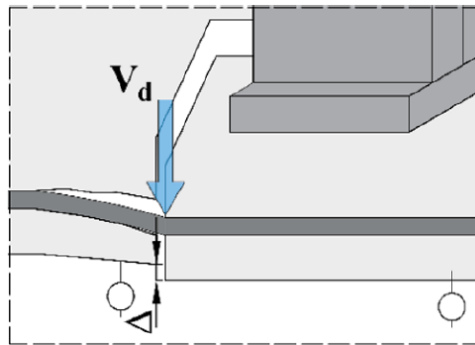


Figure 7 Dowel action effect (Lima de Resende, Cardoso, & Shehata, 2020)

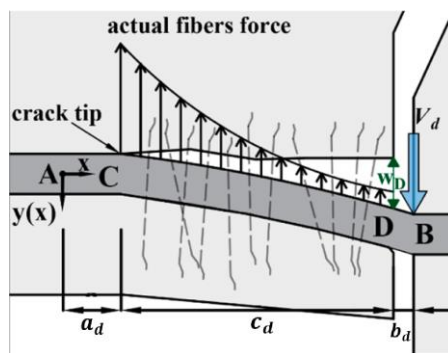


Figure 8 Actual behavior of fibers (Lima de Resende, Cardoso, & Shehata, 2020)

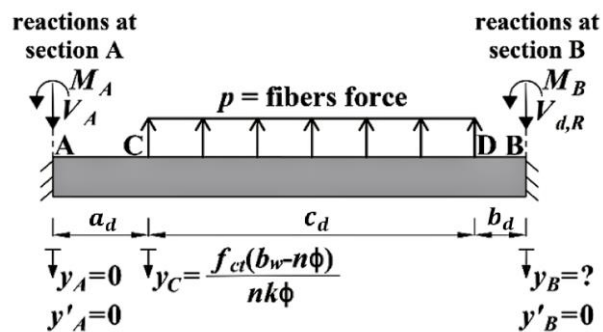


Figure 9 Proposed model (Lima de Resende, Cardoso, & Shehata, 2020)



Table 6 Equations for dowel action

Title	Equation	#	
<i>Dowel Action</i>	$c_d = a$	(54)	
	$b_d = w_b$	(55)	
	$k = \frac{E_c}{2.2 * \phi}$	(56)	
	$I_s = \frac{\pi * \left(\frac{\phi}{4}\right)^4}{4}$	(57)	
	$a_d = 1.4 * \sqrt[4]{\frac{E_s * I_s}{k * \phi}}$	(58)	
	$f_{sp} = \left( \frac{1.2 * f'_c}{20 - \sqrt{F}} + 0.7 + 1.0 * \sqrt{F} \right)$	(59)	
<i>RILEM</i>	$f_{ct} = 0.9 * f_{sp}$	(60)	
	$k_f = 1$	(61)	
	$f_{cu} = \frac{f'_c}{0.82}$	(62)	
	<i>DVB: German code</i>	$f_{Rk4} = 0.63 * \sqrt{f_{cu}} + 0.288 * \sqrt{f_{cu}} * F + 0.052 * F$	(63)
	$f_{splf} = f_{Rk4}$	(64)	
	$f_{ct} = f_{splf}$	(65)	
<i>DVB: German code</i>	$f_{ctr} = f_{splf} * 0.37$	(66)	
	$b_n = b - n_s * \phi$	(67)	
	$p = f_{ctr} * b_n$	(68)	
	$C_1 = a_d^2 c_d * (8a_d b_d^3 + 18a_d b_d^2 c_d + 12a_d b_d c_d^2 + 3a_d c_d^3 + 6b_d^3 c_d + 10b_d^2 c_d^2 + 5b_d c_d^3 + c_d^4)$	(69)	
	$C_2 = a_d^3 + 3a_d^2 d_b + 3a_d^2 c_d + 3a_d b_d^2 + 6a_d b_d c_d + 3a_d c_d^2 + 2b_d^3 + 3b_d^2 c_d + 3b_d c_d^2 + c_d^3$	(70)	

$$y_C = \frac{f_{ct} * (b_n)}{n_s * k * \phi} \quad (71)$$

$$y_B = \frac{p * C_1 + 24 * E_s * I_s * y_C * C_2}{24 * a_d^2 * E_s * I_s * (a_d + 3 * b_d + 3 * c_d)} \quad (72)$$

$$M_A = \frac{-12a_d b_d^2 c_d p - 12a_d b_d c_d^2 p - 4a_d c_d^3 p - 6b_d^2 c_d^2 p - 4b_d c_d^3 p - c_d^4 p + 72E_s I_s y_b}{12 * (a_d + b_d + c_d)^2} \quad (73)$$

$$V_A = \frac{6a_d b_d^2 c_d p + 6a_d b_d c_d^2 p + 2a_d c_d^3 p + 2b_d^3 c_d p + 6b_d^2 c_d^2 p + 4b_d c_d^3 p + c_d^4 p - 24E_s I_s y_b}{2 * (a_d + b_d + c_d)^3} \quad (74)$$

$$M_B = \frac{12a_d^2 b_d c_d p + 6a_d^2 c_d^2 p + 12a_d b_d c_d^2 p + 4a_d c_d^3 p + 4b_d c_d^3 p + c_d^4 p + 72E_s I_s y_B}{12 * (a_d + b_d + c_d)^2} \quad (75)$$

$$V_d = \frac{3 * (M_B * d_b^2 + 2 * E_s * I_s * (w_b + y_C - y_B))}{b_d^3} \quad (76)$$

$$V_d = \frac{0.5p c_d * (2a_d^3 + 6a_d^2 b_d + 6a_d^2 c_d + 6a_d b_d c_d + 4a_d c_d^2 + 2b_d c_d^2 + c_d^3) + 12E_s I_s y_B}{(a_d + b_d + c_d)^3} \quad (77)$$

$$y_D = y_B - \frac{M_B * \frac{b^2}{2} - V_d * \frac{b^3}{6}}{E_s * I_s} \quad (78)$$

$$w_D = y_D - y_C \quad (79)$$

### Height of the compression zone

The effect of the fibers for this mechanism is minimum because fibers do not increase the compression capacity in the concrete by much, they are designed to work mostly in tension. As mentioned for the aggregate interlock, the fibers will vary the internal lever arm in the flexural equilibrium, translating to a higher compression zone. The same approach used in Eq. (7) will be used to calculate the capacity the compression zone.

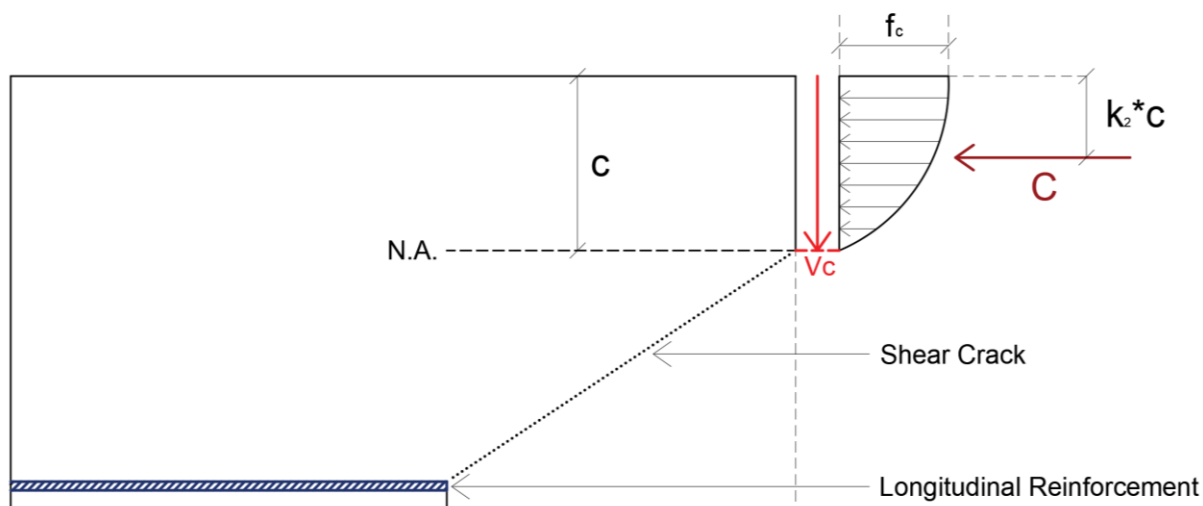


Figure 10 Direct Shear transfer in the concrete compressive zone

### Shear Capacity

The shear capacity calculated using the CSDT will be the sum of the four effects Eq. (80), in figure 10, a flow chart is shown to summarize the process. Additionally, the shear capacity due to flexion is calculated with the ultimate moment Eq. (81). Since the capacity cannot be greater than the one corresponding an ultimate state in flexion, the minimum one will determine the shear carried by the beam Eq. (82).

Table 7 Equations for shear capacity CSDT

Title	Equation	#
	$V_{CSDT} = V_c + V_d + V_{ai} + V_F$	(80)
<i>Shear capacity</i>	$V_{flexion} = \frac{M_u}{a}$	(81)
	$V = \min(V_{flexion}, V_{CSDT})$	(82)

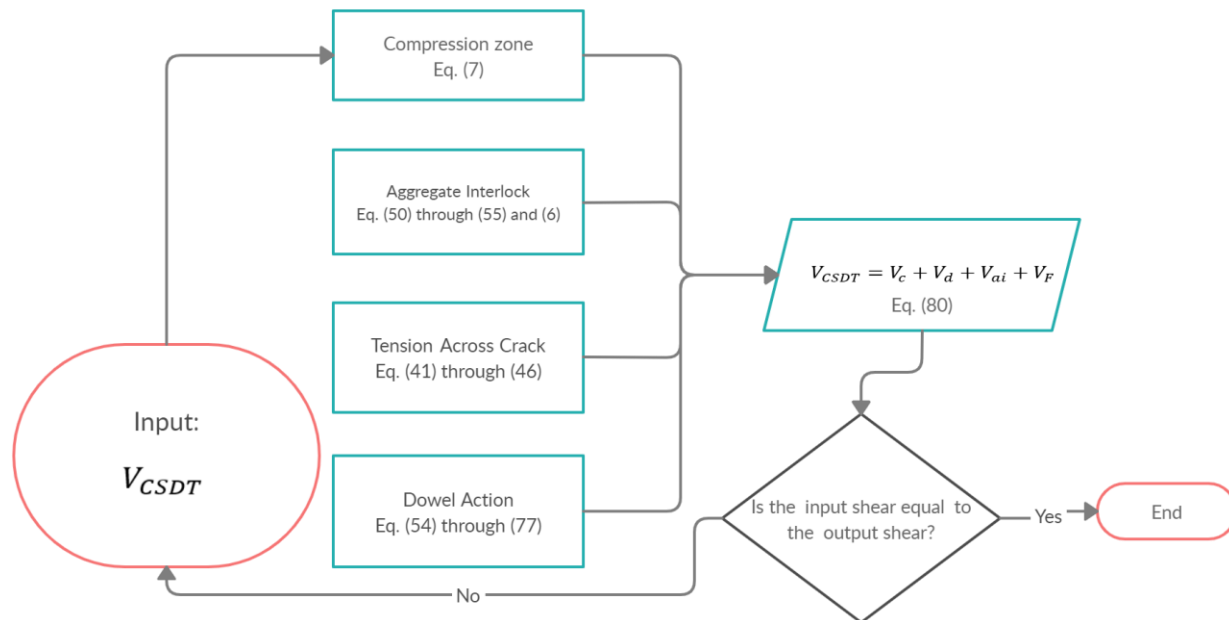


*Figure 11 Shear capacity for SFRC using CSDT*

## RESULTS

A code using Mathcad Prime 6.0.0.0 software was developed using the equations from tables 1 through 7 and the logic shown in the flow charts of figures 5 and 10 to calculate theoretically the shear carried by each mechanism along with the shear capacity using the mentioned modifications of CSDT. Table 9 shown in appendix A displays the results obtained with this code for different experimental tests. The obtained results include the shear carried by the tension across crack, aggregate interlock, dowel action and compression zone individually, as well as shear capacity. The inputs for the program were taken from a data base developed by Lantsoght (2019) and were selected using two criterions:  $a / d \geq 2.5$  and  $\rho = 1 \mp 0.5\%$ . This was done to make sure there will not be slenderness effects and the beam could reach a combined shear flexural failure. An example of the calculations with the code are shown in appendix C which inputs are taken from the results of experiment C3 done by Li, Ward, & Hamza (1992). Additionally, the ratio between the tested capacity and the predicted capacity for the experimental results is also shown in table 9. The standard deviation and the coefficient of variation for this ratio can be seen in table 8.

*Table 8 Statistical properties of tested capacity/predicted capacity for considered experiments according to different authors, with AVG = average,*

*STD = standard deviation, and COV = coefficient of variation*

<b>Tested / Predicted</b>	<b>Values</b>
<i>AVG</i>	1.05
<i>STD</i>	0.32
<i>COV</i>	30%
<i>min</i>	0.68
<i>max</i>	2.06

## DISCUSSION

The results of table 9 indicate that the capacity calculated using the modified CSDT bigger than the ones obtained from the experimental tests and shows that the results of shear capacities by looking at the ultimate moment for beams can be a very good estimation with practical ranges of rebar. This suggests that an adjustment of the expressions used in tables 1 through 7 should be made, specifically, the expressions for aggregate interlock and dowel action should be revised. In the case of aggregate interlock, the expression for the critical shear displacement  $\Delta_{cr}$  Eq. (53) should have a smaller value since fibers bridging through the shear crack will limit the overall displacement. Since Eq. (53) is an empirical expression, further experimentation is needed in order to adjust it to SFRC. In the case of dowel action, several assumptions were made in order to calculate its carried shear using the approach done by Lima de Resende, Cardoso, & Shehata (2020) such as the residual tensile strength and the crack width that should correspond to the specific configuration that was used for their equipment. The results of specimen A2.5F3.0 done by Arslan et al could not be calculated using our approach since the compressive strength of concrete  $f_c'$  was 9.77 MPa and it does not qualify as concrete since the ACI suggests that concrete elements have compressive strength of at least 17MPa. The shear capacity that is shown in table 9 used was the one calculated using equilibrium considering and ultimate flexural state, because the equilibrium assumptions imply that the beam should be able to reach this state.

The calculated capacity without CSDT shows very low error percentages and they are very consistent as the standard deviation and coefficient of variance suggest. This level of result consistency was only obtained since the data used was the one that corresponded to specimens with a low reinforcement ratio that could make the beams reach shear-flexural or even flexural failure mode. To compare the ratio of the tested capacity and predicted capacity an average of

its statistical properties according to multiple authors was done as shown in table 10 of the appendix B. In contrast to the data base predictions, the values obtained in the statistical analysis for this study present a lower standard deviation, coefficient of variance and maximum value, suggesting it could be a better approach. Additionally, all the values hover around the average, indicating that is in fact a good approximation.

The DIC approach allows the obtention of concrete strain but requires good image quality. Also, as a check and backup method the tests for SFRC should include a strain gage in the top face of the beam to measure concrete strain at any stage of the experiment. This way, no iteration will be needed and the values for the distance to the neutral axis and the strain in the longitudinal reinforcement could be derived directly.

## SUMMARY AND CONCLUSIONS

Reinforced concrete is a fundamental material in the construction sector, concrete provides resistance to compressive stress and the reinforcement of steel to tension stress. An efficient way to improve the mechanical properties of this material is by applying steel fibers in its mixture, although its use is limited by its low adoption in codes.

The aim is to determine the contribution of steel fibers in the failure mechanisms of structural elements (beams), in this case shear failure. In most codes like ACI, an empirical approach is used, so it is important to analyze a method that considers different mechanisms of contribution to the shear resistance through fibers in reinforced concrete and the direct contribution of fibers on cracking surfaces  $V_F$ . The resulting equations from this analysis will provide another method that considers the mechanical properties of the material and its specific contribution.

It was also tried to work with experimentation images (4-point test) of SFRC structural elements (beams), this through DIC, after their correction and adaptation. After the use of the Simulink method, the resulting transformations of the images did not show us the degree of correction necessary to continue the analysis, thus indicating that further investigation is required in this field.

The critical shear displacement theory was applied in this case, which considers a concrete state in which a main flexural crack reaches a critical point of stress that leads to the formation of a shear failure Crack, and therefore 2 common failure mechanisms: flexural shear failure and shear compression failure.

For the flexural shear failure state, 3 main mechanisms of shear resistance can be observed: the direct shear transfer in the concrete compressive zone  $V_C$ , the aggregate interlock



$V_{ai}$ , and the dowel action  $V_d$ . With the addition of the steel fibers, these mechanisms change because of the limitation in cracking development and the additional residual resistance of the fibers in the cracks surface. There are two defined stages in the formation of the failure system, the main critical shear crack, and the secondary cracking in the steel reinforcement, progressively increasing the width of both cracks. The shear displacement of a flexural crack is influenced by the shear, the bending moment, and the profile of the crack at the cracked cross-section. For common elements of concrete, the second failure mechanism is the most common.

In conclusion, as a result of this adaptation of the CSDT, most of the expressions now include the contribution of fibers for the different shear carrying mechanisms. Additionally, the flexural equilibrium expressions can calculate the distance to the neutral axis and the steel strain which are needed to obtain the values for the shear carrying mechanisms. These expressions are limited to sections that could reach yielding or an ultimate state and will not necessarily qualify for the CSDT, since this theory is more effective for sections that fail between cracking of the concrete and yielding of the longitudinal reinforcement.

## NOTATION LIST

- $\Delta_{cr}$  Critical shear displacement in a crack
- $A_s$  Area of the longitudinal reinforcement
- $C_1$  First simplifier factor for  $y_B$
- $C_2$  Second simplifier factor for  $y_B$
- $D_f$  Fiber bond efficiency
- $E_c$  Elastic coefficient of concrete
- $E_s$  Elastic coefficient of Steel, with a typical value of  $E_s = 200 [GPa]$
- $I_s$  Moment of inertia of the longitudinal reinforcement
- $M_A$  Reaction moment in dowel at point A
- $M_B$  Reaction moment in dowel at point B
- $M_{T,f}$  Internal moment due to fibers tension
- $M_{T,s}$  Internal moment due to longitudinal reinforcement
- $M_{ext}$  Total external moment
- $M_{int}$  Total internal moment
- $T_{f,d}$  Resultant of the fiber tension along the length of the diagonal crack
- $V_A$  Shear in dowel at point A
- $V_{CSDT}$  Total shear capacity
- $V_F$  Shear capacity due to tension across crack
- $V_{ai}$  Shear capacity due to aggregate interlock.
- $V_c$  Shear capacity in the compression zone.
- $V_d$  Shear capacity due to dowel action.
- $V_f$  Fiber Volume fraction
- $a_d$  Distance between points A and C in dowel
- $b_d$  Distance between points D and B in dowel

- $b_n$  Net width at the level of longitudinal reinforcement
- $c_d$  Distance between points C and D in dowel
- $d_f$  Equivalent diameter of the fiber
- $f_c$  Stress in the concrete in the analyzed state.
- $f_c'$  Compressive strength in concrete after 28 days of curing
- $f_{ct}$  Concrete direct tensile strength
- $f_{ctr}$  Concrete residual tensile strength
- $k_2$  ratio of the distance between the extreme compression fiber and the resultant of the compressive force to the depth of the neutral axis
- $k_c$  Slope of the stress line,  $k_c = 1.28$  according to *Krips, M.*
- $k_f$  A factor for considering the contribution of the flanges in a T-section in a stress–strain curve.
- $l_f$  Length of the fiber
- $n_e$  Ratio between elastic moduli of steel and concrete.
- $n_s$  Number of bars of longitudinal reinforcement
- $r_f$  Fiber equivalent radius
- $s_{cr}$  Height of the fully developed crack.
- $w_d$  Maximum crack opening
- $y_B$  Displacement in dowel at point B in dowel
- $y_C$  Displacement at the crack tip
- $\beta_1$  Stress block depth factor
- $\epsilon_c$  Strain of concrete in compression
- $\epsilon_o$  Strain when  $f_c$  reaches  $f_c'$
- $\epsilon_s$  Strain of Steel in tension
- $\epsilon_{sf}$  Strain in steel fibers
- $\rho_s$  Longitudinal reinforcement ratio.
- $\sigma_{fu}$  Tensile stress resisted by fibers bridging a unit area of the inclined crack.

- $\sigma_t$  Tensile Stress of SFRC
- $\Delta$  Shear displacement in a crack.
- $h$  Height of the structural Elements
- $M$  Moment in the steel reinforcement.
- $N$  Number of fibers crossing per unit area.
- $P$  External Force in the four point
- $a$  Distance from applied force to support. Equivalent Length
- $b$  Width of the structural member.
- $c$  Neutral Axis Depth
- $d$  Effective depth of the element
- $e$  Distance from the extreme compression fiber to the start of the stress block due to fibers
- $f$  Average pullout force per fiber
- $k$  modulus of elastic media
- $l$  Test span length
- $n$  Number of bars, dowel effect
- $p$  Fibers force in slitting crack.
- $w$  Crack width
- $z$  Internal lever arm.
- $\alpha$  Shear crack angle
- $\tau$  Average fiber-matrix interfacial bond strength
- $\phi$  Diameter of steel bars for Dowel action.

## BIBLIOGRAPHIC REFERENCES

- ACI Committee 363. (2010). 363R-10: Report on High-Strength Concrete. *Symposium Paper*, 65.
- ACI Committee 544. (1999). Measurement of Properties of Fiber Reinforced Concrete ACI 544.2R-89. *Symposium Paper*, 2-8.
- Anand, R., Sathya, S., & Sylviya, B. (2017). Shear strength of high-strength steel fibre reinforced concrete rectangular beams. *Int. J. Civ. Eng. Technol.*, 1716–1729.
- Aoude, H., Belghiti, M., Cook, W., & Mitchell, D. (2012). Response of Steel Fiber-Reinforced Concrete Beams with and without Stirrups. *ACI Struct. J.*, 109.
- Arslan, G., Keskin, R., & Ulusoy, S. (2017). An experimental study on the shear strength of SFRC beams without stirrups. *Theor. Appl. Mech.*, 1205–1217.
- DEUTSCHER BETON- UND BAUTECHNIK-VEREIN E.V. (2001). Stahlfaserbeton. *DBV-Merkblatt*.
- Dinh, H. H., Parra-Montesinos, G. J., & Wight, J. K. (2011). Shear Strength Model fo Steel Fiber Reinforced Concrete Beams without Stirrup Reinforcement. *Journal of Structural Engineering, ASCE*, 1039-1051.
- Kang, T.-K., Kim, W., & Massone, L. (2012). T.A. Shear-Flexure Coupling Behavior of Steel. *ACI Struct. J.*, 109.
- Krips, M. (1985). Ribbreitenbeschränkung im Stahlbeton und Spannbeton. *Mitteilungen aus dem Institut für Massivbau der Technischen Hochschule Darmstadt, Helf 33*, 84-85.
- Lantsoght, E. O. (2019). Database of Shear Experiments on Steel Fiber. *materials MDPI*, 4-6, 20-30.
- Lantsoght, E. O. (2019). How do steel fibers improve the shear capacity of reinforced concrete beams without stirrups? *ELSEVIER*.
- Li, V., Ward, R., & Hamza, A. (1992). Steel and Synthetic Fibers as Shear Reinforcement. *ACI Mater. J.*, 89.
- Lim, T., Paramasivam, P., & Lee, S. (1987). Shear and moment capacity of reinforced steel-fibre-concrete beams. *Mag. Concr. Res.*, 39, 148-160.
- Lima de Resende, T., Cardoso, D., & Shehata, L. (2020). Influence of stell fibers on the dowel action of RC beams without stirrups. *Engineering Structures*.
- MacGregor, J. G., & Wigth, J. K. (2005). *Reinforced concrete : mechanics and design*. Upper Saddle River, New Jersey: Prentice Hall.
- Mansur, M., Ong, K., & Paramasivam, P. (1986). Shear Strength of Fibrous Concrete Beams Without Stirrups. *J. Struct. Eng.*, 112, 2066–2079.
- Minelli, F., & Plizzari, G. (2013). On the Effectiveness of Steel Fibers as Shear Reinforcement. *ACI Struct. J.*, 110.
- Pratt, W. K. (2007). *DIGITAL IMAGE PROCESSING* (Fourth ed.). Los Altos, California: John Wiley & Sons, Inc. Recuperado el 14 de September de 2020

- Qissab, M., & Salman, M. (2018). Shear strength of non-prismatic steel fiber reinforced concrete beams without stirrups. *Struct. Eng. Mech.*, 67, 347–358.
- RILEM. (October de 2003).  $\sigma$ - $\epsilon$  design method Final Recommendation. (R. Committee, Ed.) *RILEM TC 162-TDF: 'Test and design methods for steel fibre reinforced concrete'*, 36, 1-6.
- Rosenbusch, J., & Teutsch, M. (2003). Trial Beams in Shear Brite/Euram Project 97-4163 Final Report Sub Task 4.2. *Technical University of Braunschweig: Braunschweig*, 105–117.
- Shoaib, A. (2012). Shear in Steel Fiber Reinforced Concrete without Stirrups. Ph.D. Thesis. *University of Alberta, Edmonton, AB, Canada*.
- Shoaib, A., Lubell, A., & Bindiganavile, V. (2015). Shear response of lightweight steel fiber reinforced concrete members without stirrups. *Mater. Struct.*, 3141-3157.
- Singh, B., & Jain, K. (2014). Appraisal of steel fibers as minimum shear reinforcement in concrete beams. *ACI Structural Journal*.
- Stahlbeton, D. A. (5 de Oktober de 2012). DAFStb-Richtlinie Stahlfaserbeton. (D. A. DAFStb, Ed.) *DEUTSCHER AUSSCHUSS FÜR STAHLBETON*, 11,12, 40.
- Thomas, J., & Ramaswamy, A. (2007). Mechanical Properties of Steel Fiber-Reinforced Concrete. *J. Mater. Civ. Eng.*, 19, 385–392.
- Thorenfeldt, E., Tomaszewicz, A., & Jensen, J. (June de 1987). Mechanical Properties of High Strength Concrete. (Trondheim, Ed.) *Proceedings of the Symposium: Utilization of High-Strength Concrete*, 149–159.
- Walraven, J. C. (1981). Fundamental Analysis of Aggregate Interlock. *Journal of Structural Engineering, ASCE*, 2245-2270.
- Wight, J. K., & MacGregor, J. G. (2012). *REINFORCED CONCRETE Mechanics and Design* (Sixth ed.). New Jersey, United States of America: Pearson Education, Inc. Retrieved Agosto 17, 2020
- Yang, Y., Uijl, J., & Walraven, J. (2016, March 02). The Critical Shear Displacement theory: on the way to extending. *Ernst & Sohn Verlag für Architektur und technische Wissenschaften*, 25. Retrieved Septiembre 12, 2020
- Zárate Garnica, G. I. (2018, October 15). Analysis of shear transfer mechanisms in concrete members without shear reinforcement based on kinematic measurements. *Master of Science in Structural Engineering Thesis*, 92. Retrieved Septiembre 25, 2020

## APENDIX A

*Table 9 Results for SFRC using CSDT*

ID	Author	a/d	$\rho$	$c_y$ [mm]	c [mm]	Mext [kN-m]	Mint [kN-m]	V_F [kN]	V_ai [kN]	V_d [kN]	V_c [kN]	V_CSDT [kN]	V_flexion [kN]	Shear Capacity [kN]	Vu [kN]	Tested Capacity/Predicted Capacity
L62	Shoab, Lubell and Bindiganavile. 2015	3.000	0.012	213.060	242.102	509	509	223	50	403	445	929	249	249	306	1.23
SH4	Manju et al. 2017	2.500	0.013	60.330	59.910	28	28	43	8	82	39	170	55	55	63	1.13
SH5		2.500	0.013	62.050	60.688	35	35	86	9	96	52	242	60	60	79	1.31
SH6		2.500	0.013	63.620	61.636	59	59	128	9	109	67	313	65	65	135	2.06
A2.5F1.0A	Arslan et al. 2017	2.500	0.013	77.670	89.046	33	33	39	5	76	44	164	63	63	65	1.03
A2.5F1.0b		2.500	0.013	86.450	79.225	22	22	36	10	65	45	156	60	60	44	0.73
A2.5F2.0		2.500	0.013	94.110	90.420	25	25	61	8	73	60	203	60	60	50	0.83
A2.5F3.0		2.500	0.013	-	-	20	20	-	-	-	-	-	46	46	39	0.85
A3.5F1.0		3.500	0.013	94.115	103.556	32	32	26	9	82	51	168	34	34	33	0.97
A3.5F2.0		3.500	0.013	94.110	94.100	30	30	59	6	102	71	238	43	43	43	0.99
A3.5F3.0		3.500	0.013	85.396	95.539	41	41	100	5	135	94	334	47	47	59	1.26
A4.5F1.0		4.500	0.013	86.465	97.857	39	39	30	5	115	61	212	33	33	43	1.27
A4.5F2.0	4.500	0.013	94.111	103.556	32	32	54	5	130	80	268	34	34	35	1.04	
2.3/2	Rosenbusch and Teutsch. 2003	2.500	0.012	89.673	75.999	53	53	29	29	118	56	233	112	112	82	0.73
2.3/3		2.500	0.012	91.463	90.771	70	70	80	22	134	76	310	114	114	107	0.94
A0.5%	Aoude et al. 2012	2.970	0.012	88.641	88.351	29	29	16	4	66	33	119	49	49	48	0.97
A1%		2.970	0.012	94.519	102.086	34	34	27	3	70	40	140	49	49	57	1.15
B0.5%		3.089	0.015	212.000	180.509	214	214	71	46	246	165	528	227	227	154	0.68
B1%		3.089	0.015	226.255	223.922	273	273	114	36	263	191	602	225	225	198	0.88
NSC1-FRC1	Minelli & Plizzari. 2013	2.506	0.010	168.627	160.290	145	145	38	26	157	77	298	163	163	129	0.79
NSC2-FRC1		2.506	0.010	151.110	127.823	129	129	50	37	183	85	354	170	170	115	0.68
NSC2-FRC2		2.506	0.010	150.824	141.455	153	153	35	20	179	74	308	169	169	137	0.81
NSC3-FRC		2.506	0.010	145.623	133.834	153	153	52	34	196	86	368	172	172	136	0.79
HSC1-FRC1		2.506	0.010	137.589	153.472	207	207	100	17	259	100	476	185	185	186	1.00
NSC4-FRC-500-1		2.505	0.010	175.263	199.259	223	223	23	15	159	67	264	174	174	194	1.12
NSC4-FRC-500-2		2.505	0.010	175.264	171.430	177	177	26	24	159	71	279	174	174	154	0.89
NSC4-FRC-1000		2.500	0.010	355.270	326.216	575	575	53	107	165	112	435	349	349	247	0.71
HSC2-FRC-1000		2.500	0.010	285.038	270.298	759	759	87	142	247	129	601	384	384	328	0.85
2/0.5/2.5	Lim et al. 1987	2.500	0.012	81.399	78.336	32	32	28	12	78	40	157	67	67	58	0.87
B2	Mansur et al. 1986	2.800	0.014	79.753	78.226	29	29	21	9	71	39	140	59	59	53	0.89
B3		3.600	0.014	79.753	107.090	32	32	16	7	90	44	157	46	46	45	0.98
C2		2.800	0.014	79.360	90.760	33	33	29	5	76	42	153	60	60	60	1.01
C6		2.800	0.014	95.796	93.191	25	25	23	8	63	41	135	56	56	45	0.81
M15	Li, Ward, Hamza. 1992	3.000	0.011	61.985	36.335	4	4	5	0	25	8	39	11	11	13	1.19
C3		3.000	0.011	42.615	48.160	5	5	7	1	18	9	35	10	10	16	1.61
FNB-50-1	Kang et al. 2012	2.548	0.011	108.083	123.860	105	105	52	16	161	72	301	117	117	131	1.12
G1B5	Qissab and Salman. 2018	2.500	0.011	50.273	72.180	14	14	11	2	34	16	64	25	25	41	1.62
G1B6		2.500	0.011	50.356	67.188	18	18	17	2	36	18	74	25	25	51	2.00
N10-1	Shoab. 2012	3.000	0.014	351.495	436.466	1351	1351	375	241	378	361	1346	508	508	479	0.94
H10-1		3.000	0.014	330.712	334.601	1777	1777	634	150	527	390	1700	561	561	633	1.13

## APENDIX B

*Table 10 Statistical properties of tested capacity/predicted capacity for considered experiments according to different authors, with **AVG** = average,*

*STD = standard deviation, and COV = coefficient of variation*

<b>Authors</b>	<b>Sarveghadi et al</b>	<b>Kwak et al</b>	<b>Greenough and Nehdi</b>	<b>Khuntia et al</b>	<b>Imam et al</b>	<b>Sharma</b>	<b>Mansur et al</b>	<b>Ashour et al 1</b>	<b>Ashour et al 2</b>	<b>Arslan et al</b>	<b>Yakoub et al 1</b>	<b>Yakoub et al 2</b>	<b>Average</b>
<i>AVG</i>	0.76	0.84	1.07	1.22	1.07	0.85	0.87	0.75	1.21	1.07	1.79	2.55	1.17
<i>STD</i>	0.25	0.24	0.38	0.36	0.42	0.23	0.32	0.22	0.37	0.29	0.68	1.18	0.41
<i>COV</i>	33%	29%	35%	29%	39%	28%	37%	29%	31%	27%	38%	46%	34%
<i>min</i>	0.21	0.34	0.33	0.59	0.32	0.56	0.25	0.24	0.47	0.70	1.06	1.09	0.51
<i>max</i>	1.27	1.40	2.03	2.21	2.51	1.43	1.77	1.28	2.15	1.85	4.34	6.26	2.37



## APENDIX C

### MathCAD Code

#### Inputs:

$f'_c = 22.7 \text{ MPa}$	Compression Strength of Concrete	$\rho_f = 1$	fiber bond efficiency
$f_y = 450 \text{ MPa}$	Yield strength of Steel	$V_f = 1$	fiber volume fraction
$A_s = 0.713 \text{ cm}^2$	Area of steel	$d_f = 0.5 \text{ mm}$	fiber equivalent diameter
$E_s = 200 \text{ GPa}$	Steel elastic Modulus	$l_f = 30 \text{ mm}$	fiber length
$b = 63.5 \text{ mm}$	Section thickness	$\alpha := 30 \text{ deg}$	crack inclination
$d = 102 \text{ mm}$	effective depth	$l = 71.2 \text{ cm}$	span length
$h = 127 \text{ mm}$	Height of beam	$M_{ext} = 4.82535 \text{ kN} \cdot \text{m}$	External Moment
$a = 306 \text{ mm}$	distance from P to supp.	$\phi = 9.53 \text{ mm}$	Diameter of bars
$n_s = 1$	Number of bars		

#### Flexion Equilibrium (finds c):

- Finding Cracking Moment:

$$RI := \frac{\left(\frac{V_f}{100} \cdot l_f\right)}{d_f} = 0.6 \quad \text{mechanical properties of SFRC - Job thomas}$$

$$f_{rf} := \left( 0.97 \cdot \left(\frac{f'_c}{0.82}\right)^{0.5} + 0.295 \cdot \left(\frac{f'_c}{0.82}\right)^{0.5} \cdot RI + 1.117 \cdot RI \right) \cdot \text{MPa} = 6.705 \text{ MPa}$$

$$E_c := 4700 \cdot \sqrt{\frac{f'_c}{\text{MPa}}} \cdot \text{MPa} = (2.23929 \cdot 10^4) \text{ MPa} \quad I_g := \frac{(b \cdot h^3)}{12}$$

$$\varepsilon_{cr} := \frac{f_{rf}}{E_c} = 0.0003 \quad \varepsilon_{s,cr} := \frac{\left(\frac{d-h}{2}\right)}{\left(\frac{h}{2}\right)} \cdot \varepsilon_{cr} = 1.81544 \cdot 10^{-4}$$

$$M_{cr} := \frac{(f_{rf} \cdot I_g)}{\left(\frac{h}{2}\right)} = 1.14455 \text{ kN} \cdot \text{m} \quad \phi_{cr} := \frac{\varepsilon_{s,cr}}{\frac{h}{2}} = 0.003 \frac{1}{m}$$

- Finding Yield Moment with Thorenfeldt approach:

$$c_y := 70 \text{ mm} \quad \text{Iterate this value until } T_y = C_y$$

$$n := 0.8 + \left( \frac{f'_c}{2500 \text{ psi}} \right) = 2.117 \quad \varepsilon_o := \frac{f'_c}{E_c} \cdot \left( \frac{n}{n-1} \right) = 0.00192$$

$$\varepsilon_y := \frac{f_y}{E_s} = 0.00225 \quad \varepsilon_{c,y} := \frac{\varepsilon_y}{d - c_y} \cdot c_y = 0.00492$$

$$\beta_{1,y} := \frac{\ln \left( 1 + \left( \frac{\varepsilon_{c,y}}{\varepsilon_o} \right)^2 \right)}{\left( \frac{\varepsilon_{c,y}}{\varepsilon_o} \right)} = 0.79 \quad k_{2,y} := 1 - \frac{2 \cdot \left( \left( \frac{\varepsilon_{c,y}}{\varepsilon_o} \right) - \text{atan} \left( \frac{\varepsilon_{c,y}}{\varepsilon_o} \right) \right)}{\left( \frac{\varepsilon_{c,y}}{\varepsilon_o} \right)^2 \cdot \beta_{1,y}} = 0.474 \quad \text{Thorenfeldt}$$

$$F := \left( \frac{l_f}{d_f} \right) \cdot \frac{V_f}{100} \cdot \rho_f = 0.6$$

$$\sigma_t := \begin{cases} \text{if } f'_c \geq 55 \text{ MPa} \\ \quad \left| \begin{array}{l} 2 \text{ MPa} \cdot F \\ \text{if } f'_c < 55 \text{ MPa} \\ \quad 0.772 \text{ MPa} \cdot F \end{array} \right. \end{cases} = 0.463 \text{ MPa}$$

ACI Committee 544 (1988)  
ACI Committee 363: High  
strength concrete 363r ()

$$\varepsilon_{sf} := \frac{\sigma_t}{E_c} = 0.00002 \frac{\text{mm}}{\text{mm}}$$

$$e_y := (\varepsilon_{sf} + \varepsilon_{c,y}) \cdot \left( \frac{c_y}{\varepsilon_{c,y}} \right) = 70.29419 \text{ mm}$$

$$k := \begin{cases} \text{if } \left( \frac{\varepsilon_{c,y}}{\varepsilon_o} \right) \leq 1 \\ \quad \left| \begin{array}{l} 1 \\ \text{if } \left( \frac{\varepsilon_{c,y}}{\varepsilon_o} \right) > 1 \\ \quad 0.67 + \frac{f'_c}{9000 \text{ psi}} \end{array} \right. \end{cases} = 1.036$$

$$f_c := \frac{0.9 \cdot f'_c \cdot n \cdot \left( \frac{\varepsilon_{c,y}}{\varepsilon_o} \right)}{n - 1 + \left( \frac{\varepsilon_{c,y}}{\varepsilon_o} \right)^{n \cdot k}} = 12.332 \text{ MPa}$$

$$A_s = 0.713 \text{ cm}^2 \quad A_s \cdot f_y = 32.099 \text{ kN} \quad \sigma_t \cdot b \cdot (h - e_y) = 1.668 \text{ kN}$$

$$C_y := \beta_{1,y} \cdot f_c \cdot b \cdot c_y = 43.292 \text{ kN} \quad \text{within 2\%}$$

$$T_y := A_s \cdot f_y + \sigma_t \cdot b \cdot (h - e_y) = 33.767 \text{ kN}$$

$$M_y := (A_s \cdot f_y \cdot (d - k_{2,y} \cdot c_y)) + \sigma_t \cdot b \cdot (h - e_y) \cdot \left( \frac{h}{2} + \frac{e_y}{2} - k_{2,y} \cdot c_y \right) = 2.31823 \text{ kN} \cdot \text{m}$$

$$\phi_y := \frac{\varepsilon_y}{d - c_y} = 0.07 \frac{1}{\text{m}} \quad \varepsilon_y = 0.002$$

- Finding Ultimate Moment:

$$\beta_{1w} := \begin{cases} \text{if } f'_c \leq 28 \text{ MPa} & 0.85 \\ \text{if } f'_c \geq 55 \text{ MPa} & 0.65 \\ \text{if } 28 \text{ MPa} < f'_c < 55 \text{ MPa} & 0.85 - \left( 0.05 \cdot \frac{f'_c - 28 \text{ MPa}}{7 \text{ MPa}} \right) \end{cases} = 0.85$$

$$c_1 := c_w \cdot \beta_{1w} \cdot b \cdot f'_c \cdot 0.85 = A_s \cdot \left( E_s \cdot \frac{0.003 \cdot (d - c_w)}{c_w} \right) + \sigma_t \cdot b \cdot \left( h - (\varepsilon_{sf} + 0.003) \cdot \left( \frac{c_w}{0.003} \right) \right) \xrightarrow{\text{solve, } c_w, \text{float, } 6} \dots$$

$$c_1 = \begin{bmatrix} 48.16 \\ -84.631 \end{bmatrix} \text{ mm} \quad c_u := c_{1_0} = 48.16 \text{ mm}$$

$$e_u := (\varepsilon_{sf} + 0.003) \cdot \left( \frac{c_u}{0.003} \right) = 48.492 \text{ mm}$$

$$a_u := \frac{A_s \cdot f_y + \sigma_t \cdot b \cdot (h - e_u)}{0.85 \cdot f'_c \cdot b} = 28.083 \text{ mm}$$

$$M_u := \left( A_s \cdot f_y \cdot \left( d - \frac{a_u}{2} \right) \right) + \sigma_t \cdot b \cdot (h - e_u) \cdot \left( \frac{h}{2} + \frac{e_u}{2} - \frac{a_u}{2} \right) = 2.99356 \text{ kN} \cdot \text{m}$$

$$\varepsilon_{su} := \frac{0.003 \cdot (d - c_u)}{c_u} = 0.003 \quad \phi_u := \frac{\varepsilon_{su}}{d - c_u} = 0.062 \frac{1}{\text{m}}$$

- Finding steel strain corresponding to  $M_{ext}$  (using  $M-\phi$  linear interpolation):

$$A_M := \begin{bmatrix} M_{cr} \\ M_y \\ M_u \end{bmatrix} \quad B_\phi := \begin{bmatrix} \phi_{cr} \\ \phi_y \\ \phi_u \end{bmatrix} \quad \phi_{M_{ext}} := \text{linterp}(A_M, B_\phi, M_{ext}) = 0.041 \frac{1}{m}$$

$$c := 18.5 \text{ mm} \quad \text{Iterate this value until } M_{ext} = M_{int}$$

$$\varepsilon_s := \phi_{M_{ext}} \cdot (d - c) = 0.003385 \frac{\text{mm}}{\text{mm}}$$

- Finding internal moment:

$$\varepsilon_c := \frac{\varepsilon_s}{d - c} \cdot c = 0.00075 \frac{\text{mm}}{\text{mm}} \quad e := (\varepsilon_{sf} + \varepsilon_c) \cdot \left( \frac{c}{\varepsilon_c} \right) = 19.01024 \text{ mm}$$

$$f_s := \varepsilon_s \cdot E_s = 677.016 \text{ MPa}$$

$$\beta_1 := \frac{\ln \left( 1 + \left( \frac{\varepsilon_c}{\varepsilon_o} \right)^2 \right)}{\left( \frac{\varepsilon_c}{\varepsilon_o} \right)} = 0.363 \quad k_2 := 1 - \frac{2 \cdot \left( \left( \frac{\varepsilon_c}{\varepsilon_o} \right) - \text{atan} \left( \frac{\varepsilon_c}{\varepsilon_o} \right) \right)}{\left( \frac{\varepsilon_c}{\varepsilon_o} \right)^2 \cdot \beta_1} = 0.343 \quad \text{Thorenfeldt}$$

$$M_{T_{steel}} := A_s \cdot f_s \cdot (d - k_2 \cdot c) = 4.61948 \text{ kN} \cdot \text{m}$$

$$M_{T_{fiber}} := \sigma_t \cdot b \cdot (h - e) \cdot \left( \frac{h}{2} + \frac{e}{2} - k_2 \cdot c \right) = 0.21174 \text{ kN} \cdot \text{m}$$

$$M_{int} := M_{T_{steel}} + M_{T_{fiber}} = 4.831 \text{ kN} \cdot \text{m}$$

$$M_{ext} = 4.825 \text{ kN} \cdot \text{m}$$

- Strain and c for  $M_{ext} > M_u$

$$\varepsilon_s := \begin{cases} \text{if } M_{ext} \geq M_u \\ \varepsilon_{su} \\ \text{if } M_{ext} < M_u \\ \varepsilon_s \end{cases} = 0.003 \quad c := \begin{cases} \text{if } M_{ext} \geq M_u \\ c_u \\ \text{if } M_{ext} < M_u \\ c \end{cases} = 48.16 \text{ mm}$$

### Tension Across Crack (Finds $V_F$ ):

$$\tau := 0.85 \cdot \sqrt{\frac{f'_c}{\text{MPa}}} \cdot \text{MPa} \quad \text{average fiber-matrix interfacial bond strength}$$

$$f := \tau \cdot \pi \cdot \rho_f \cdot d_f \cdot \frac{l_f}{4} = 0.04771 \text{ kN} \quad \text{Average pullout force per fiber}$$

$$r_f := \frac{d_f}{2} \quad \text{fiber equivalent radius}$$

$$N := 0.5 \cdot \frac{100}{\pi \cdot r_f^2} \quad \text{number of fibers crossing per unit area}$$

$$\sigma_{fu} := N \cdot f \quad \text{tensile stress resisted by fibers bridging a unit area of the inclined crack}$$

$$V_F = T_{f_d} \cdot \cos(\alpha)$$

$T_{f_d}$  = resultant of the fiber tension along the length of the diagonal crack

$$V_F := \sigma_{fu} \cdot b \cdot (d - c) \cdot \cot(\alpha) = 7.19442 \text{ kN}$$

### Aggregate interlock (finds $V_{ai}$ ):

- Simplified Crack Properties

$$n_e := \frac{E_s}{E_c} = 8.931$$

$$\rho_r := \frac{A_s}{2.5 \cdot (h - d) \cdot b} = 0.018 \quad \text{effective reinforcement ratio (Euro code)}$$

$$k_{1f} := 1 + 2 \sqrt{\frac{200}{d}} = 2.4 \quad \text{a coefficient which takes account of the bond properties of the bars} \quad k_{2f} := 0.5 \quad \text{bending}$$

$$l_{crm} := \left( 50 \text{ mm} + 0.25 k_{1f} \cdot k_{2f} \cdot \frac{\phi}{\rho_r} \right) \cdot \left( \frac{50}{\left( \frac{l_f}{d_f} \right)} \right) = 174.242 \text{ mm} \quad \text{CHANGE WITH RILEM AND GERMAN CODE}$$

$$s_{cr} := \left( 1 + \rho_s \cdot n_e - \sqrt{2 \cdot \rho_s \cdot n_e + (\rho_s \cdot n_e)^2} \right) \cdot d = 65.693 \text{ mm}$$

- Crack width at the level of longitudinal reinforcement

$$w_b := l_{crm} \cdot \varepsilon_s = 0.584 \text{ mm}$$

- Critical Shear Displacement

$$\Delta_{cr} := \left\| \begin{array}{l} \text{if } \left( \frac{25 d}{30610 \phi} + 0.0022 \right) \leq 0.025 \\ \left\| \left( \frac{25 d}{30610 \phi} + 0.0022 \right) \right. \\ \text{if } \left( \frac{25 d}{30610 \phi} + 0.0022 \right) > 0.025 \\ \left\| 0.025 \right. \end{array} \right\| = 0.011 \quad \text{d and } \phi \text{ in mm}$$

- Shear carried by aggregate interlock

$$V_{ai} := \left( \frac{f'_c}{\text{MPa}} \right)^{0.56} \cdot \text{MPa} \cdot s_{cr} \cdot b \cdot \frac{0.03 \text{ mm}}{w_b - 0.01 \text{ mm}} \left( -978 \Delta_{cr}^2 + 85 \cdot \Delta_{cr} - 0.27 \right) = 0.68 \text{ kN}$$

$$V_{ai} = 0.68 \text{ kN}$$

### Dowel Action (finds $V_d$ ):

- Finding fibers force along splitting crack:

$$c_d := a = 30.6 \text{ cm}$$

we assume is equal to a (distance from P to support)

$$b_d := w_b = 0.584 \text{ mm}$$

we assume is equal to wb (main crack width)

$$I_s := \frac{\pi \cdot \left(\frac{\phi}{2}\right)^4}{4}$$

$$k := \frac{E_c}{2.2 \cdot \phi}$$

$$a_d := 1.4 \cdot \sqrt[4]{\frac{E_s \cdot I_s}{k \cdot \phi}} = 1.322 \text{ cm}$$

$$f_{sp} := \left( \frac{1.2 \cdot \frac{f'_c}{\text{MPa}}}{20 - \sqrt{F}} + 0.7 + 1.0 \cdot \sqrt{F} \right) \cdot \text{MPa} = 2.891 \text{ MPa}$$

$$f_{ct} := 0.9 f_{sp} = 2.602 \text{ MPa}$$

### RILEM

$$k_f := 1 \quad \begin{array}{l} \text{factor for taking into account the} \\ \text{contribution of the} \\ \text{flanges in a T-section} \end{array}$$

$$f_{cu} := \frac{f'_c}{0.82} \quad \text{Ultimate Concrete strength}$$

### DVB: German code.

$$f_{Rk4} := \left( 0.63 \cdot \sqrt[2]{\frac{f_{cu}}{\text{MPa}}} + 0.288 \cdot \sqrt[2]{\frac{f_{cu}}{\text{MPa}}} \cdot F + 0.052 \cdot F \right) \cdot \text{MPa} = 4.255 \text{ MPa}$$

Thomas, J.; Ramaswamy, A. Mechanical Properties of Steel Fiber-Reinforced Concrete. J. Mater. Civ. Eng. **2007**, 19, 385–392. [CrossRef]

Residual tensile strengths of CMOD: 3,5 [mm]

$$f_{splf} := f_{Rk4} = 4.255 \text{ MPa}$$

$$\tau_{fd} := 0.12 \cdot f_{splf}$$

design value of the increase in shear strength due to steel fibres

$$V_{fd} := 0.7 \cdot k_f \cdot k_{1f} \cdot \tau_{fd} \cdot b \cdot d = 5.557 \text{ kN} \quad \text{contribution of the steel fiber shear reinforcement according to RILEM code}$$

$$f_{ctr} := f_{splf} = 4.255 \text{ MPa}$$

$$f_{ctr} := f_{splf} \cdot 0.37 = 1.574 \text{ MPa} \quad \text{DAfStb relation}$$

$$b_n := b - n_s \cdot \phi = 53.97 \text{ mm}$$

$$p := f_{ctr} \cdot b_n = 84.97 \frac{\text{kN}}{\text{m}} \quad \text{fibers force between splitting crack}$$

- Finding Moments on dowel:

$$C_1 := a_d^2 \cdot c_d \cdot (8 \cdot a_d \cdot b_d^3 + 18 \cdot a_d \cdot b_d^2 \cdot c_d + 12 \cdot a_d \cdot b_d \cdot c_d^2 + 3 \cdot a_d \cdot c_d^3 + 6 \cdot b_d^3 \cdot c_d + 10 \cdot b_d^2 \cdot c_d^2 + 5 \cdot b_d \cdot c_d^3 + c_d^4) = (5.348 \cdot 10^{-7}) \text{ m}^7$$

$$C_2 := a_d^3 + 3 a_d^2 b_d + 3 a_d^2 c_d + 3 a_d b_d^2 + 6 a_d b_d c_d + 3 a_d c_d^2 + 2 b_d^3 + 3 b_d^2 c_d + 3 b_d c_d^2 + c_d^3 = 0.033 \text{ m}^3$$

$$y_C := \frac{f_{ct} \cdot (b_n)}{n_s \cdot k \cdot \phi} = 0.014 \text{ mm}$$

$$y_B := \frac{p \cdot C_1 + 24 E_s \cdot I_s \cdot y_C \cdot C_2}{24 a_d^2 \cdot E_s \cdot I_s \cdot (a_d + 3 b_d + 3 c_d)} = 14.612 \text{ cm}$$

$$M_A := \frac{-12 \cdot a_d \cdot b_d^2 \cdot c_d \cdot p - 12 \cdot a_d \cdot b_d \cdot c_d^2 \cdot p - 4 a_d \cdot c_d^3 \cdot p - 6 \cdot b_d^2 \cdot c_d^2 \cdot p - 4 \cdot b_d \cdot c_d^3 \cdot p - c_d^4 \cdot p + 72 \cdot E_s \cdot I_s \cdot y_B}{12 \cdot (a_d + b_d + c_d)^2} = -0.023 \text{ kN} \cdot \text{m}$$

$$V_A := \frac{6 \cdot a_d \cdot b_d^2 \cdot c_d \cdot p + 6 \cdot a_d \cdot b_d \cdot c_d^2 \cdot p + 2 a_d \cdot c_d^3 \cdot p + 2 \cdot b_d^3 \cdot c_d \cdot p + 6 \cdot b_d^2 \cdot c_d^2 \cdot p + 4 \cdot b_d \cdot c_d^3 \cdot p + c_d^4 \cdot p - 24 \cdot E_s \cdot I_s \cdot y_B}{2 \cdot (a_d + b_d + c_d)^3} = 8.124 \text{ kN}$$

$$M_B := \frac{12 \cdot a_d^2 \cdot b_d \cdot c_d \cdot p + 6 \cdot a_d^2 \cdot c_d^2 \cdot p + 12 \cdot a_d \cdot b_d \cdot c_d^2 \cdot p + 4 \cdot a_d \cdot c_d^3 \cdot p + 4 \cdot b_d \cdot c_d^3 \cdot p + c_d^4 \cdot p + 72 \cdot E_s \cdot I_s \cdot y_B}{12 \cdot (a_d + b_d + c_d)^2} = 1.418 \text{ kN} \cdot \text{m}$$

Finding Shear carried by dowel action:

$$V_d := \frac{0.5 p \cdot c_d \cdot (2 \cdot a_d^3 + 6 \cdot a_d^2 \cdot b_d + 6 \cdot a_d^2 \cdot c_d + 6 \cdot a_d \cdot b_d \cdot c_d + 4 a_d \cdot c_d^2 + 2 \cdot b_d \cdot c_d^2 + c_d^3) + 12 \cdot E_s \cdot I_s \cdot y_B}{(a_d + b_d + c_d)^3} = 17.876 \text{ kN}$$

$$V_d = 17.876 \text{ kN}$$



$$y_D := y_B - \frac{M_B \cdot \frac{b^2}{2} - V_d \cdot \frac{b^3}{6}}{E_s \cdot I_s} = 12.023 \text{ cm}$$

$$w_D := y_D - y_C = 12.022 \text{ cm}$$

### Height of the compression zone

$$V_{total} := 35.238 \text{ kN}$$

iterate this value until  $V_{total} = V_{csdt}$

$$V_c := \frac{d - s_{cr}}{d + 0.5 \cdot s_{cr}} \cdot V_{total} = 9.488 \text{ kN}$$

$$V_c = 9.4876 \text{ kN}$$

### Shear capacity:

$$V_{CSDT} := V_c + V_d + V_{ai} + V_F = 35.238 \text{ kN}$$

$$V_{flexion} := \frac{M_u}{a} = 9.783 \text{ kN}$$

$$V := \min(V_{flexion}, V_{CSDT}) = 9.783 \text{ kN}$$

Calculated value

$$V_u = 15.739 \text{ kN} \quad \text{Real Value}$$

$$error := \text{abs}\left(\frac{V_u - V}{V_u}\right) = 0.378$$